Positivity statements for a mixed-element-volume scheme on fixed and moving grids

Paul-Henry Cournède[*] — Bruno Koobus[**] — Alain Dervieux[***]

[*] *LMAS, Ecole Centrale Paris, F-92295 Châtenay-Malabry*
paul-henry.cournede@mas.ecp.fr

[**] *Mathématiques, Université de Montpellier II, CC 051, F-34095 Montpellier*
koobus@math.univ-montp2.fr

[***] *INRIA, 2003 Route des Lucioles, F-06902 Sophia-Antipolis*
Alain.Dervieux@inria.fr

ABSTRACT. *This paper considers a class of second-order accurate vertex-centered mixed finite-element finite-volume MUSCL schemes. These schemes apply to unstructured triangulations and tetrahedrizations and fluxes are computed on an edge basis. We define conditions under which these schemes satisfy a density-positivity statement for Euler flows, a maximum principle for a scalar conservation law and a multicomponent flow. This extends to an Arbitrary-Lagrangian-Eulerian formulation. Steady and unsteady flow simulations illustrate the accuracy and the robustness of these schemes.*

RÉSUMÉ. *On considère une classe de schémas mixtes-eléments-volumes centrés-sommets, et décentrés par une méthode MUSCL. Ces schémas s'appliquent à des triangulations et tétraèdrisations non structurées et les flux sont calculés par arêtes. On donne des conditions suffisantes pour que ces schémas vérifient la positivité de la masse volumique pour le modèle des équations d'Euler, le principe du maximum pour les lois de conservations scalaires et pour les écoulements multicomposants. Ceci s'étend à du Euler-Lagrange arbitraire. Des calculs d'écoulements stationnaires et instationnaires illustrent la précision et la robustesse de ces schémas.*

KEYWORDS: *finite-element, finite-volume, positivity, maximum principle, scalar conservation law, Euler, ALE, multi-component, fluid-structure interaction.*

MOTS-CLÉS : *éléments finis, volumes finis, positivité, principe du maximum, loi de conservation scalaire, Euler, ALE, multicomposant, interaction fluide-structure.*

1. Introduction

Some of the most useful contributions of upwind approximation schemes for hyperbolic equations are their monotonicity and positivity properties. For example, for the Euler equations, and by combining flux splitting and limiters, Perthame and coworkers ((Perthame *et al.*, 1992), (Perthame *et al.*, 1996)) have proposed second-order accurate schemes that maintain a density and a temperature positive. We refer also to (Linde *et al.*, 1998) and to the workshop (Venkatakrisnan, 1998). Non-oscillating schemes ((Harten *et al.*, 1987),(Cockburn *et al.*, 1989)) propose high accuracy approximations applicable to many problems. However, they do not enjoy a strict satisfaction of positivity or monotony, which remains an important issue for stiff simulations, particularly in relation with highly heterogeneous fluid flows (see for example (Abgrall, 1996), (Murrone *et al.*, 2005)).

The purpose of the present work is to state several positivity results for a set of schemes refered as mixed-element-volume (MEV) methods. Some of these properties, like second-order accurate monotony for variable meshes were, as far as we know, not stated for any other scheme, but we think the proposed proof can extend to many other schemes. Concerning the MEV method, it is a family of approximations that have been and are still intensively used to solve complex flow problems of industrial type, including calculations on moving meshes. MEV is both a Finite-Element method (FEM) and a Finite-Volume method (FVM). The underlying FEM is the standard Galerkin method with continuous piecewise linear approximation on triangles or tetrahedra. The FEM is applied directly on second-order derivatives (diffusion or viscosity terms). For hyperbolic terms, the FEM needs extra stabilization terms which are derived from an upwind FVM. The underlying FVM is a vertex centered edge-based one. The finite-volume cell is built around each vertex, generally by using medians (2D) or median planes (3D), advection terms are stabilized with upwinding or artificial dissipation, and second order "viscous" terms are discretized with finite-elements. This family of schemes was initiated by Baba and Tabata (Baba *et al.*, 1981) for diffusion-convection problems and Fezoui *et al.* (see (Fezoui *et al.*, 1989b),(Fezoui *et al.*, 1989a),(Stoufflet *et al.*, 1996)) for Euler flows. It has been studied by many CFD teams (see in particular (Catalano, 2002),(Whitaker *et al.*, 1989), (Venkatakrishnan, 1996)). Lastly, the framework proposed in (Selmin *et al.*, 1998) can be considered as an extension of MEV.

Current developements and results relying on this family of schemes are regularly reported by Farhat and co-workers (see (Farhat *et al.*, 2000)). In (Farhat *et al.*, 2001), in particular, the authors demonstrate the crucial role of the so-called Discrete Geometric Conservation Law in the positivity of the ALE version of a first-order-accurate MEV method. The work we propose here concentrates on the second-order accurate MEV schemes, extending in particular the results of (Farhat *et al.*, 2001).

Among the different ways of constructing second-order accurate positive schemes, the MUSCL formulation introduced by Van Leer in (Van Leer, 1979) for finite volume methods is particularly attractive. It is based on the application of the Godunov method to flow values that result from cell-wise higher-order interpolation. The advantage of MUSCL is its modularity, and the possibility of improving the accuracy of the scheme by improving the cell reconstruction; it was early proven to be TVD in 1D linear case (Sweby, 1984). Derivations of vertex-centered MUSCL second-order accurate schemes on unstructured meshes appeared in the mid of 80's (see e.g. (Fezoui *et al.*, 1989b)). The positivity of the first-order versions in the case of advection models dates back to (Baba *et al.*, 1981). Robustness issues for *second-order* versions were not met before the so-called "upwind triangle derivative" was introduced (Stoufflet *et al.*, 1996) and successfully applied to stiff high Mach number flow calculations. But a complete mathematical analysis of the reason of this robustness was not derived at that time (see however the discussions in (Fezoui *et al.*, 1989a) and (Arminjon *et al.*, 1993)).

Positivity of vertex-centered schemes has been addressed by very few authors. Considering schemes that are not of finite-volume type, an element-wise limitation is introduced in MDHR (Multi-Dimensional High Resolution) approximations, by Sidilkover in (Sidilkover, 1994) and Deconinck *et al.* in (Deconinck *et al.*, 1993); it leads to positivity statements for advection. Positivity of a triangular, vertex-centered version of the Nessyahu-Tadmor scheme is shown in (Arminjon *et al.*, 1999). Concerning genuine finite-volume methods involving *edgewise interpolation and limitation*, recent improvements for steady flows with proofs restricted to linear case have been proposed in (Piperno *et al.*, 1998). A notable contribution was brought by Jameson in (Jameson, 1993); this author proposed a LED (Local Extremum Diminishing) scheme based on the "upwind-triangle derivative". The Jameson LED scheme is of symmetric-TVD type (thus not a MUSCL scheme), which means that for each flux, a unique limiter determines the convenient blending of two (symmetric) schemes.

In the present paper, we derive and study a genuinely MUSCL adaptation of the Jameson LED limiter: the interpolation limitation is realized thanks to the so-called upwind triangle, and an extra interpolation may give a high-order asymptotic accuracy (*i.e.* far from extrema). The purpose is to give a proof of the nonlinear stability for the scheme introduced in (Stoufflet *et al.*, 1996) and for some variants.

Our strategy is first to show the maximum principle for a scalar conservation law, then to introduce a flux splitting that preserves density positivity for the Euler equations. This provides a basis to construct multidimensional schemes that ensure density positivity and maximum principle for convected species. This is of paramount importance for most flows of industrial interest for two reasons. A direct one is that most industrial flows are at medium Mach number and they generally do not induce negative pressures but more often negative densities that can arise at after bodies (negative pressures are more often obtained in high Mach number detached shocks). The second reason is that in many Reynolds-Averaged Navier-Stokes flows, limiters are not necessary for the mean flow itself, but robustness problems arise in the computation of turbulence closure variables such as k and ε. Larrouturou derived in (Larrouturou, 1991) a second-order 1D scheme and a first-order 2D (and 3D) scheme for multi-component flows that preserves the maximum principle. In the present work, we extend Larrouturou's approach and define a high-order scheme on 2D-3D unstructured meshes that preserves the maximum principle for passive advective variables.

The paper is organised as follows. In Section 2, a scalar nonlinear model is considered and allows us to introduce the main features of the new scheme. In Section 3, the well-known positivity 1D statements for the Euler equations are reformulated in such a way that we can derive the extension of the new scheme to density-positive treatment of the 2D and 3D Euler equations. Section 4 is devoted to the maximum principle for passive species. The last section is devoted to a sample of numerical applications.

In order to keep the discussion within reasonable bounds, we consider in our analysis only explicit time advancing.

2. Positive schemes and LED schemes for nonlinear scalar conservation laws

This section recalls some useful existing results. We keep the usual TVD/LED criterion preferably to weaker positivity criteria in order to deal also with the maximum principle.

2.1. *Nonlinear scalar conservation laws in fixed and moving domains*

Fixed domains: We consider a nonlinear scalar conservation law in Euler form for the unknown $U(\mathbf{x},t)$:

$$\frac{\partial U}{\partial t}(\mathbf{x},t) + \nabla_{\mathbf{x}} \cdot \mathcal{F}\Big(U(\mathbf{x},t)\Big) = 0 \qquad [1]$$

where t denotes the time, $\mathbf{x} = (x_1, x_2, x_3)^t$ is the space coordinate and $\mathcal{F}(U) = (F(U), G(U), H(U))^t$ (3D case). Under some classical assumptions (Godlewski *et al.*, 1996), the solution U satisfies a *maximum principle* that, for simplicity, we write in the case of the whole space:

$$\min_{\mathbf{x}} U(\mathbf{x},0) \leq U(\mathbf{x},t) \leq \max_{\mathbf{x}} U(\mathbf{x},0) \qquad [2]$$

Moving domains: We consider a nonlinear scalar conservation law in ALE form for the unknown $U(\mathbf{x},t)$. Similar notations to (Farhat *et al.*, 2001) are used. We denote an instantaneous configuration by $\Omega(\mathbf{x},t)$ where $\mathbf{x} = (x_1,x_2,x_3)^t$ is the 3D space coordinate and t the time, and a reference configuration by $\Omega(\xi, \tau = 0)$ where $\xi = (\xi_1, \xi_2, \xi_3)^t$ denotes the space coordinate and τ the time. We have a map function $\mathbf{x} = \mathbf{x}(\xi,\tau), t = \tau$, from $\Omega(\xi,\tau=0)$ to $\Omega(\mathbf{x},t)$, and $J = det(\partial\mathbf{x}/\partial\xi)$ denotes its determinant. Then, the nonlinear scalar conservation law in ALE form can be written as :

$$\frac{\partial JU}{\partial t}|_{\xi}(\mathbf{x},t) \; + \; J\,\nabla_{\mathbf{x}} \cdot \Big(\mathcal{F}(U(\mathbf{x},t)) - \mathbf{w}(\mathbf{x},\mathbf{t})U(\mathbf{x},t)\Big) = 0 \qquad [3]$$

where $\mathcal{F}(U) = (F(U), G(U), H(U))^t \quad and \quad \mathbf{w} = \frac{\partial \mathbf{x}}{\partial t}|_{\xi}$. As for fixed domain problems, the solution U satisfies a *maximum principle*.

2.2. *Positivity/LED criteria*

Assuming that the mesh nodes are numbered, we call U_i the value at mesh node i that can move in time for moving grids. We recall now the classical positivity statement for an explicit time-integration (the proof is immediate).

Lemma 1 *A positivity criterion: suppose that an explicit first-order time-integration of Equation [1] or [3] can be expressed in the form:*

$$\frac{U_i^{n+1} - U_i^n}{\Delta t} = b_{ii} U_i^n + \sum_{j \neq i} b_{ij} U_j^n \ , \qquad [4]$$

where all the b_{ij}, $j \neq i$, are non-negative and $b_{ii} \in \mathbb{R}$. Then it can be shown that the above explicit scheme preserves positivity under the following condition on the time-step Δt: $b_{ii} + \dfrac{1}{\Delta t} \geq 0$.

REMARK. — Under a possibly different restriction on Δt, a high-order explicit time discretization can still preserve the positivity, see (Shu *et al.*, 1988). □

Another scheme formulation relies on the so-called incremental form that dates back to Harten (Harten, 1983). It was used by Jameson in (Jameson, 1993) for defining Local Extremum Diminishing (LED) schemes (see also (Godlewski *et al.*, 1996)). We recall now the theory introduced by Jameson (Jameson, 1993) on LED schemes in the case of an explicit time-integration:

Lemma 2 *A LED criterion (Jameson, 1993): suppose that an explicit first-order time-integration of Equation [1] or [3] can be written in the form:*

$$\frac{U_i^{n+1} - U_i^n}{\Delta t} = \sum_{k \in V(i)} c_{ik}(U^n)\,(U_k^n - U_i^n)\,. \qquad [5]$$

with all the $c_{ik}(U^n) \geq 0$, and where $V(i)$ denotes the set of the neighbours of node i. Then the previous scheme verifies that a local maximum cannot increase and a local minimum cannot decrease, and under an appropriate condition on the time-step the positivity and the maximum principle are preserved.

Proof: given U_i^n a local maximum, we deduce that $(U_k^n - U_i^n) \leq 0$ for all $k \in V(i)$. Therefore [5] implies that $\dfrac{U_i^{n+1} - U_i^n}{\Delta t} \leq 0$, and the local maximum cannot increase. Likewise, we can prove that a local minimum cannot decrease. On the other hand, the reader can easily check that the positivity and the maximum principle are preserved when the time-step satisfies $\dfrac{1}{\Delta t} - \displaystyle\sum_{k \in V(i)} c_{ik}(U^n) \geq 0$. □

2.3. *First-order space-accurate MEV schemes on fixed and moving grids*

In this work, we use a vertex-centred finite-volume approximation on a dual mesh constructed from a finite element discretization of the computational domain by triangles (2D) or tetrahedra (3D). In the 2D case, the cells are delimited by the triangle medians (see Figure 1), and in 3D the cells are delimited by planes through the middle of an edge (see Figure 2). In the case of moving grids, these cells can move and deform with time according to vertices motion.

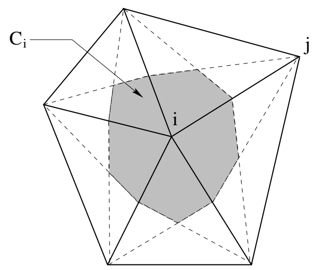

Figure 1. *The finite volume cell Ω_i (2D case)*

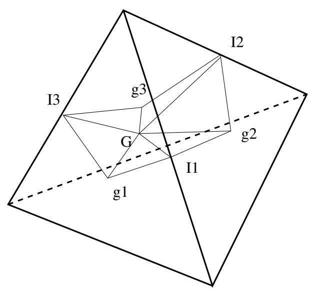

Figure 2. *The planes which delimit finite volume cells inside a tetrahedron (3D case)*

Fixed grids: Integrating [1] over a cell Ω_i, integrating by parts the resulting convective fluxes and using a conservative approximation leads to the following semi-discretization of [1]:

$$a_i \frac{dU_i}{dt} + \sum_{j \in V(i)} \Phi(U_i, U_j, \nu_{ij}) = 0 \qquad [6]$$

where a_i is the measure of cell Ω_i, $V(i)$ is the set of nodes connected to node i, and $\nu_{ij} = \int_{\partial\Omega_{ij}} \mu_{ij}\, ds$ in which μ_{ij} denotes the unitary normal to the boundary $\partial\Omega_{ij} = \partial\Omega_i \cap \partial\Omega_j$ shared by the cells Ω_i and Ω_j. In the above semi-discretization, the values U_i and U_j correspond to a constant per cell *interpolation* of the variable U, and Φ is a *numerical flux function* so that $\Phi(U_i, U_j, \nu_{ij})$ approximates $\displaystyle\int_{\partial\Omega_{ij}} \mathcal{F}(U) \cdot \mu_{ij}(s)ds$. In general, the numerical flux function $\Phi\ :\ (u, v, \nu) \rightarrow \Phi(u, v, \nu)$ is assumed to be Lipschitz continuous, monotone increasing with respect to u, monotone decreasing with respect to v, and consistent:

$$\Phi(u, u, \nu) = \mathcal{F}(u) \cdot \nu\ . \qquad [7]$$

Moving grids: Integrating [3] over a cell $\Omega_i(0)$ of the ξ space, switching to the $\mathbf{x}$ space, integrating by part the resulting convective fluxes and using a conservative approximation lead to the following semi-discretization of [3]:

$$\frac{d\Big(a_i(t)U_i\Big)}{dt} + \sum_{j\in V(i)} \Phi(U_i, U_j, \nu_{ij}(t), \kappa_{ij}(t))\ =\ 0 \qquad [8]$$

where $a_i(t)$ is the measure of cell $\Omega_i(t)$, $\nu_{ij}(t)\ =\ \displaystyle\int_{\partial\Omega_{ij}(t)} \mu_{ij}(s,t)\, ds$ and

$\kappa_{ij}(t)\ =\ \displaystyle\int_{\partial\Omega_{ij}(t)} \mathbf{w}(s,t) \cdot \mu_{ij}(s,t)\, ds$. In the above semi-discretized scheme, Φ is *a numerical flux function* so that $\Phi(U_i, U_j, \nu_{ij}(t), \kappa_{ij}(t))$ approximates $\displaystyle\int_{\partial\Omega_{ij}(t)} (\mathcal{F}(U) - \mathbf{w}U) \cdot \mu_{ij} ds$. As previously, $\Phi\ :\ (u, v, \nu, \kappa)\ \mapsto\ \Phi(u, v, \nu, \kappa)$ is assumed to be Lipschitz continuous, monotone increasing with respect to u, monotone decreasing with respect to v, and consistent:

$$\Phi(u, u, \nu, \kappa) = \mathcal{F}(u) \cdot \nu - \kappa u\ . \qquad [9]$$

2.4. *Limited high-order space-accurate MEV scheme on fixed and moving grids*

In this paper, high-order MEV schemes are derived according to the MUSCL method of Van Leer (Van Leer, 1979). In this approach, the order of space-accuracy is improved by substituting in the numerical flux function, the values U_i and U_j by "better" interpolations U_{ij} and U_{ji} at the interface $\partial\Omega_{ij}$. More precisely, the first-order MEV scheme becomes:

$$a_i \frac{dU_i}{dt} + \sum_{j\in V(i)} \Phi(U_{ij}, U_{ji}, \nu_{ij})\ =\ 0 \quad \text{in the case of } \textit{fixed grids}, \qquad [10]$$

and

$$\frac{d\Big(a_i(t)U_i\Big)}{dt} + \sum_{j\in V(i)} \Phi(U_{ij}, U_{ji}, \nu_{ij}(t), \kappa_{ij}(t))\ =\ 0 \quad \text{for } \textit{moving grids}, \qquad [11]$$

where U_{ij} and U_{ji} are left and right values of U at the interface $\partial\Omega_{ij}$ (see Figure 3 for the 2D case) obtained by interpolation. In order to keep the scheme non oscillatory

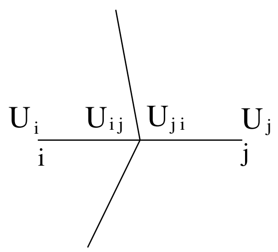

Figure 3. *Interface values U_{ij} and U_{ji} between vertices i and j.*

and positive, we have to introduce *limiters*. It has been proved early that high-order positive schemes must be necessarily built with a nonlinear process. In the case of unstructured meshes and scalar models, second-order positive schemes were derived using a two-entry symmetric limiter by Jameson in (Jameson, 1993). Here, instead of a symmetric limiter, we choose a MUSCL formulation (involving two limiters per edge) according to Van Leer (Van Leer, 1979). The adaptation to triangulations is close to the one proposed in (Fezoui *et al.*, 1989a) and (Stoufflet *et al.*, 1996). From the upwind schemes proposed by these authors, we introduce three-entry limiters, following (Debiez, 1996); this allows us to design a positive scheme, of third- (or even fifth-) order far from extrema when U varies smoothly. Then [10] becomes for *fixed grids*:

$$a_i \frac{dU_i}{dt} + \sum_{j \in V(i)} \Phi(U_i + \frac{1}{2} L_{ij}(U), U_j - \frac{1}{2} L_{ji}(U), \nu_{ij}) \;=\; 0, \qquad [12]$$

and [11] becomes for *moving grids*:

$$\frac{d(a_i(t)U_i)}{dt} + \sum_{j \in V(i)} \Phi(U_i + \frac{1}{2} L_{ij}(U), U_j - \frac{1}{2} L_{ji}(U), \nu_{ij}(t), \kappa_{ij}(t)) \;=\; 0. \quad [13]$$

In order to define $L_{ij}(U)$ and $L_{ji}(U)$ we use the upstream and downstream triangles (or tetrahedra) T_{ij} and T_{ji} (see Figures 4 and 5), as introduced in (Fezoui *et al.*, 1989a). Element T_{ij} is *upstream* to vertex i with respect to edge ij if for any small enough real number η the vector $-\eta\vec{ij}$ is inside element T_{ij}. Symmetrically, element T_{ji} is *downstream* to vertex i with respect to edge ij if for any small enough real number η the vector $\eta\vec{ji}$ is inside element T_{ij}. Let ϵ_{ri}, ϵ_{si}, ϵ_{ti}, ϵ_{jn}, ϵ_{jp} and ϵ_{jq} be the components of vector $\vec{ji}$ (resp. $\vec{ij}$) in the oblique system of axes $(\vec{ir}, \vec{is}, \vec{it})$ (resp. $\vec{jn}, \vec{jp}, \vec{jq}$)):

$$\vec{ji} \;=\; \epsilon_{ri}\,\vec{ir} \,+\, \epsilon_{si}\,\vec{is} \,+\, \epsilon_{ti}\,\vec{it}\,,$$
$$\vec{ij} \;=\; \epsilon_{jn}\,\vec{jn} \,+\, \epsilon_{jp}\,\vec{jp} \,+\, \epsilon_{jq}\,\vec{jq}\,.$$

Then T_{ij} and T_{ji} are upstream and downstrean elements means that they have been chosen in such a way that the components ϵ_{ri}, etc. are all nonnegative: T_{ij} upstream and T_{ji} downstream $\Leftrightarrow$ $\epsilon_{ri}, \epsilon_{si}, \epsilon_{ti}, \epsilon_{jn}, \epsilon_{jp}, \epsilon_{jq}$ are all non-negative. Let us introduce the following notations:

$$\Delta^- U_{ij} \;=\; \vec{\nabla} U\,|_{T_{ij}}\,.\,\vec{ij} \quad , \quad \Delta^0 U_{ij} = U_j - U_i \quad and \quad \Delta^- U_{ji} \;=\; \vec{\nabla} U\,|_{T_{ji}} \cdot \vec{ij}\,,$$

where the gradients are those of the P1 (continuous and linear) interpolation of U.

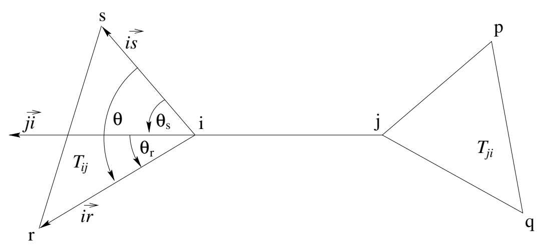

Figure 4. *Downstream and Upstream triangles are triangles having resp. i and j as a vertex and such that line ij intersects the opposite edge*

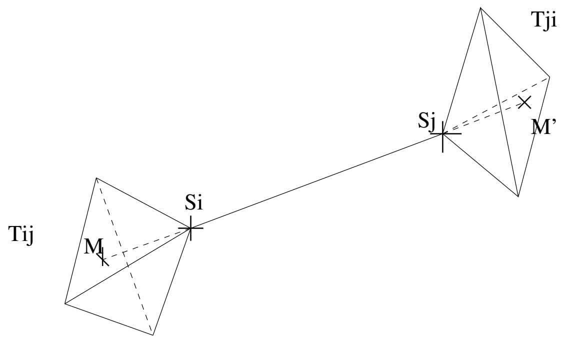

Figure 5. *Downstream and Upstream tetrahedra are tetrahedra having resp. S_i and S_j as a vertex and such that line S_iS_j intersects the opposite face*

Jameson in (Jameson, 1993) has noted that (for the 3D case):

$$\Delta^- U_{ij} \;=\; \epsilon_{ri}\,(U_i \,-\, U_r) \,+\, \epsilon_{si}\,(U_i \,-\, U_s) \,+\, \epsilon_{ti}\,(U_i \,-\, U_t)\,,$$

and

$$\Delta^- U_{ji} \;=\; \epsilon_{jp}\,(U_p \,-\, U_j) \,+\, \epsilon_{jq}\,(U_q \,-\, U_j) \,+\, \epsilon_{jn}\,(U_n \,-\, U_j)\,,$$

with the same non-negative ϵ_{ri}, ϵ_{si}, ϵ_{ti}, ϵ_{jn}, ϵ_{jp} and ϵ_{jq}.
Now, we introduce a family of continuous limiters with three entries, satisfying:

$(P1)$ $L(u,v,w) \;=\; L(v,u,w)$
$(P2)$ $L(\alpha\, u, \alpha\, v, \alpha\, w) \;=\; \alpha\, L(v,u,w)$
$(P3)$ $L(u,u,u) \;=\; u$
$(P4)$ $L(u,v,w) \;=\; 0$ if $uv \leq 0$
$(P5)$ $0 \leq \frac{L(u,v,w)}{v} \leq 2$ if $v \neq 0$.

Note that there exists K^- and K^0 depending on (u,v,w) such that:

$$L(u,v,w) = K^- u = K^0 v \;,\; \text{with } 0 \leq K^- \leq 2 \;,\; 0 \leq K^0 \leq 2 \,. \qquad [14]$$

A function verifying (P1) to (P5) exists, and in the numerical examples, we shall use the following version of the Superbee method of Roe:

$$\left\{ \begin{array}{lcll} L_{SB}(u,v,w) & = & 0 & \text{if} \;\; uv \leq 0 \\ & = & Sign(u)\, \min(\, 2\,|u|\,,\, 2\,|v|\,,\, |w|) & \text{otherwise.} \end{array} \right. \qquad [15]$$

We define:

$$L_{ij}(U) = L(\Delta^- U_{ij}\,,\, \Delta^0 U_{ij}\,,\, \Delta^{HO} U_{ij}) \;;\; L_{ji}(U) = L(\Delta^- U_{ji}\,,\, \Delta^0 U_{ij}\,,\, \Delta^{HO} U_{ji}). \qquad [16]$$

where $\Delta^{HO} U_{ji}$ is a third way of evaluating the variation of U which we can introduce for increasing the accuracy of the resulting scheme (see the following remark).

REMARK. — Let assume that the option $L_{ij}(U) \;=\; \Delta^{HO}\, U_{ij}$ gives a high order approximation with order ω. For U smooth enough and assuming that the mesh size is smaller than α (small), there exists $\epsilon(\alpha)$ such that if $\dfrac{|\vec{\nabla} U . \vec{ij}|}{||\vec{ij}||} > \epsilon(\alpha)$ for an edge ij, the limiter L_{ij} is not active, *i.e.* $L_{ij}(U) = \Delta^{HO}\, U_{ij}$. Then, the scheme is locally of order ω.$\square$

REMARK. — Second-order accuracy of MEV in case of arbitrary unstructured meshes is difficult to state in general. We refer to (Mer, 1998) for proofs in simplified cases. $\square$

The proposed analysis does not need any assumption concerning the terms $\Delta^{HO} U_{ij}$. For example, we can use the following flux:

$$\Delta^{HO3} U_{ij} = \frac{1}{3}\, \Delta^- U_{ij} + \frac{2}{3}\, \Delta^0 U_{ij} \,, \qquad [17]$$

which gives us a third-order space-accurate scheme for linear advection on cartesian triangular meshes. More generally, the high-order flux can use extra data in order to increase the accuracy. In (Debiez *et al.*, 1998) and (Camarri *et al.*, 2004), the following version is studied:

$$\begin{aligned}\Delta^{HO5}U_{ij} &= \Delta^{HO3}U_{ij} \\ &\quad -\frac{1}{30}\left[\Delta^{-}U_{ij} - 2\Delta^{0}U_{ij} + \Delta^{-}U_{ji}\right] \\ &\quad -\frac{2}{15}\left[(\vec{\nabla}U)_M.\vec{ij} - 2(\vec{\nabla}U)_i.\vec{ij} + (\vec{\nabla}U)_j.\vec{ij}\right] . \end{aligned} \qquad [18]$$

For a vertex k, the notation $(\vec{\nabla}U)_k$ holds for the following average of the gradients on tetrahedra T having the node k as a vertex:

$$(\vec{\nabla}U)_k = -\frac{1}{Vol(C_k)}\sum_{T,k\in T}\frac{Vol(T)}{4}\vec{\nabla}U|_T \qquad [19]$$

The term $(\vec{\nabla}U)_M$ is the gradient at point M, intersection of line ij with the face of T_{ij} that does not have i as vertex, see Figure 5 (3D case). It is computed by linear interpolation of the nodal gradient values at the vertices contained in the face opposite to i in the upwind tetrahedron T_{ij}. This option gives fifth-order accuracy for the linear advection equation on cartesian meshes and has a dissipative leading error expressed in terms of sixth-order derivatives.

2.5. *Maximum principle for first-order space-accurate MEV schemes on fixed and moving grids*

Fixed grids: the first-order explicit time-integration of [6] leads to the following scheme:

$$\frac{U_i^{n+1} - U_i^n}{\Delta t} = \sum_{j\in V(i)} c_{ij}\,(U_j^n - U_i^n) + d_i\,U_i^n \qquad [20]$$

where the coefficients:

$$c_{ij} = -\frac{1}{a_i}\,\frac{\Phi(U_i^n, U_j^n, \nu_{ij}) - \Phi(U_i^n, U_i^n, \nu_{ij})}{U_j^n - U_i^n} \qquad [21]$$

are always positive since the flux Φ is monotone decreasing with respect to the second variable. The last term in [20] involves:

$$d_i = -\frac{1}{a_i}\,\frac{\displaystyle\sum_{j\in V(i)}\Phi(U_i^n, U_i^n, \nu_{ij})}{U_i^n} \qquad [22]$$

which, due to the consistent condition [7], can be transformed as follows:

$$d_i = -\frac{1}{a_i}\,\frac{1}{U_i^n}\,\mathcal{F}(U_i^n)\,.\sum_{j\in V(i)}\nu_{ij}\,. \qquad [23]$$

Therefore this term vanishes since the finite-volume cells are closed:

$$\sum_{j\in V(i)} \nu_{ij} \;=\; 0,\;\; \forall\; i\,. \qquad [24]$$

According to Lemma 2, we conclude classically that the scheme resulting from the first-order explicit time-integration of [6] is L^∞-stable under the CFL condition:

$$\frac{1}{\Delta t} \;-\; \sum_{j\in V(i)} c_{ij} \;\geq\; 0. \qquad [25]$$

Moving grids: the maximum principle has been extended to *ALE formulations* by Farhat *et al.* in (Farhat *et al.*, 2001) for first-order space-accurate schemes. We recall this in short. The time-integration of [8] is obtained by combining a given time-integration scheme for fixed grid with a procedure for evaluating the geometric quantities that arise from the ALE formulation. Since the mesh configuration changes in time, an important problem is the correct computation of the numerical flux function Φ through the evaluation of the geometric quantities $\nu_{ij}(t)$ and $\kappa_{ij}(t)$. In order to address this problem, the discrete scheme is required to preserve a constant solution. In the case of a first-order explicit time-integration of [8], imposing this condition to the discrete scheme leads to the following relation called the *Discrete Geometric Conservation Law (DGCL)*:

$$a_i^{n+1} \;-\; a_i^n = \Delta t \sum_{j\in V(i)} \bar{\kappa}_{ij} \qquad [26]$$

with $a_i^n \;=\; |\Omega_i^n|$ and $a_i^{n+1} \;=\; |\Omega_i^{n+1}|$, and where $\bar{\kappa}_{ij}$ is a time-averaged value of $\kappa_{ij}(t)$. This gives a procedure for the evaluation of the geometric quantities in the numerical flux function based on a combination of suited mesh configurations.
Then the first-order space-accurate ALE scheme [8] combined with a first-order explicit time-integration can be written as follows:

$$\frac{a_i^{n+1}U_i^{n+1} - a_i^n U_i^n}{\Delta t} \;+\; \sum_{j\in V(i)} \Phi(U_i^n, U_j^n, \bar{\nu}_{ij}, \bar{\kappa}_{ij}) \;=\; 0\,. \qquad [27]$$

where $\bar{\nu}_{ij}$ and $\bar{\kappa}_{ij}$ are averaged value of $\nu_{ij}(t)$ and $\kappa_{ij}(t)$ on suited mesh configurations so that the numerical scheme satisfies the DGCL. Given that $\sum_{j\in V(i)} \bar{\nu}_{ij} = 0$ since the cells Ω_i remain closed during the mesh motion, the consistency condition [9] implies that:

$$\Phi(U_i^n, U_i^n, \bar{\nu}_{ij}, \bar{\kappa}_{ij}) = \Phi(U_i^n, U_i^n, \bar{\nu}_{ij}, \bar{\kappa}_{ij}) - \sum_{j\in V(i)} \mathcal{F}(U_i^n)\cdot\bar{\nu}_{ij} = -\sum_{j\in V(i)} \bar{\kappa}_{ij} U_i^n.$$

Then, the above scheme can also be written as:

$$\frac{U_i^{n+1} \;-\; U_i^n}{\Delta t} \;\;=\;\; \sum_{j\in V(i)} c_{ij}\;(U_j^n - U_i^n) \;+\; e_i U_i^n\;, \qquad [28]$$

$$c_{ij} \;=\; -\,\frac{1}{a_i^{n+1}}\,\frac{\Phi(U_i^n, U_j^n, \bar{\nu}_{ij}, \bar{\kappa}_{ij}) \;-\; \Phi(U_i^n, U_i^n, \bar{\nu}_{ij}, \bar{\kappa}_{ij})}{U_j^n - U_i^n}\,, \qquad [29]$$

$$e_i \;=\; \left(\frac{a_i^n - a_i^{n+1}}{a_i^{n+1}\Delta t} \;+\; \frac{1}{a_i^{n+1}}\sum_{j\in V(i)} \bar{\kappa}_{ij}\right)\,. \qquad [30]$$

We note again that the coefficients c_{ij} are always positive since the numerical flux function Φ is monotone decreasing with respect to the second variable. We observe also that the DGCL [26] is exactly the condition for which e_i defined by [30] vanishes. As for the fixed grids case, from Lemma 2 we conclude that the ALE scheme [27] is L^∞-stable under the CFL condition:

$$\frac{1}{\Delta t} \;-\; \sum_{j\in V(i)} c_{ij} \;\geq\; 0. \qquad [31]$$

2.6. *Maximum principle for limited high-order space-accurate MEV scheme on fixed and moving grids*

Fixed grids: a first-order explicit time-integration of the high-order upwind scheme given by Equation [10] leads to the following equation:

$$\frac{a_i U_i^{n+1} - a_i U_i^n}{\Delta t} \;+\; \sum_{j\in V(i)} \Phi(U_{ij}^n, U_{ji}^n, \nu_{ij}) \;=\; 0\,. \qquad [32]$$

Lemma 3 *The scheme defined by [32] combined with [15], [16] and [17] or [18] satisfies the maximum principle under an appropriate CFL condition.*

Proof: let us first introduce the following coefficients:

$$g_{ij} \;=\; -\,\frac{1}{a_i}\,\frac{1}{U_{ji}^n - U_i^n}\,\big(\Phi(U_{ij}^n, U_{ji}^n, \nu_{ij}) \;-\; \Phi(U_{ij}^n, U_i^n, \nu_{ij})\big) \qquad [33]$$

$$h_{ij} \;=\; -\,\frac{1}{a_i}\,\frac{1}{U_{ij}^n - U_i^n}\,\big(\Phi(U_{ij}^n, U_i^n, \nu_{ij}) \;-\; \Phi(U_i^n, U_i^n, \nu_{ij})\big) \qquad [34]$$

$$d_i \;=\; -\,\frac{1}{a_i}\,\frac{1}{U_i^n}\left(\sum_{j\in V(i)} \Phi(U_i^n, U_i^n, \nu_{ij})\right)\,. \qquad [35]$$

Then, the scheme [32] can be written as:

$$\frac{U_i^{n+1} - U_i^n}{\Delta t} \;=\; \sum_{j\in V(i)} g_{ij}\,(U_{ji}^n - U_i^n) \;+\; \sum_{j\in V(i)} h_{ij}\,(U_{ij}^n - U_i^n) \;+\; d_i\,U_i^n \qquad [36]$$

We can notice that the coefficients g_{ij} and h_{ij} are respectively positive and negative since the numerical flux function Φ is monotone increasing with the first variable and monotone decreasing with the second variable. As in the previous section, the term d_i vanishes since the numerical flux function Φ satisfies the consistency condition [7] and the finite-volume cells Ω_i are closed so that identity [24] holds. On the other hand, according to [14] and [16] we can write $L_{ij}(U^n)$ as:

$$L_{ij}(U^n) = K_{ij}^- \Delta^- U_{ij}^n$$

where K_{ij}^- is a positive function of U^n , so that we have:

$$U_{ij}^n - U_i^n = \frac{1}{2} L_{ij}(U^n) = \frac{1}{2} K_{ij}^- \Big(\epsilon_{ri}(U_i^n - U_r^n) + \epsilon_{si}(U_i^n - U_s^n) + \epsilon_{ti}(U_i^n - U_t^n) \Big) . \qquad [37]$$

Likewise, from [14] and [16] we can write $L_{ji}(U^n)$ in the following form:

$$L_{ji}(U^n) = K_{ji}^0 \Delta^0 U_{ij}^n$$

where K_{ji}^0 is a positive function of U^n smaller than 2, so that we get:

$$U_{ji}^n - U_i^n = U_j^n - \frac{1}{2} L_{ji}(U^n) - U_i^n = \Big(1 - \frac{K_{ji}^0}{2} \Big) (U_j^n - U_i^n) \qquad [38]$$

in which the coefficient $1 - \dfrac{K_{ji}^0}{2}$ is positive. In the idendity [36], we substitute $U_{ij}^n - U_i^n$ and $U_{ji}^n - U_i^n$ respectively by their expressions given by [37] and [38], so that we can write the discrete upwind scheme in the following form:

$$\frac{U_i^{n+1} - U_i^n}{\Delta t} = \sum_{j \in V(i)} \alpha_{ij} (1 - \frac{K_{ji}^0}{2}) (U_j^n - U_i^n) + \sum_{j \in V(i)} \beta_{ij} (U_j^n - U_i^n) \qquad [39]$$

where the coefficients α_{ij} and β_{ij} are positive, so that this scheme satisfies the maximum principle under a CFL condition according to Lemma 2.

Moving grids: A first-order explicit time-integration of the high-order upwind scheme given by [11] leads to the following equation:

$$\frac{a_i^{n+1} U_i^{n+1} - a_i^n U_i^n}{\Delta t} + \sum_{j \in V(i)} \Phi(U_{ij}^n, U_{ji}^n, \overline{\nu}_{ij}, \overline{\kappa}_{ij}) \; = \; 0 \, . \qquad [40]$$

where $\overline{\nu}_{ij}$ and $\overline{\kappa}_{ij}$ are averaged value of $\nu_{ij}(t)$ and $\kappa_{ij}(t)$ on suited mesh configurations so that the numerical scheme satisfies the DGCL [26].

Lemma 4 *The scheme defined by [40] combined with [15], [16] and [17] or [18] satisfies the maximum principle under an appropriate CFL condition.*

Proof: let first introduce the following coefficients:

$$g_{ij} \;\; = \;\; - \frac{1}{a_i^{n+1}} \, \frac{\Phi(U_{ij}^n, U_{ji}^n, \overline{\nu}_{ij}, \overline{\kappa}_{ij}) \; - \; \Phi(U_{ij}^n, U_i^n, \overline{\nu}_{ij}, \overline{\kappa}_{ij})}{U_{ji}^n - U_i^n} \qquad [41]$$

$$h_{ij} \;=\; -\frac{1}{a_i^{n+1}}\,\frac{\Phi(U_{ij}^n,U_i^n,\bar{\nu}_{ij},\bar{\kappa}_{ij}) \;-\; \Phi(U_i^n,U_i^n,\bar{\nu}_{ij},\bar{\kappa}_{ij})}{U_{ij}^n - U_i^n}\,, \qquad [42]$$

$$e_i \;=\; \left(\frac{a_i^n - a_i^{n+1}}{a_i^{n+1}\Delta t} \;+\; \frac{1}{a_i^{n+1}}\sum_{j\in V(i)} \bar{\kappa}_{ij}\right). \qquad [43]$$

Then, the scheme defined by [40] becomes:

$$\frac{U_i^{n+1} \;-\; U_i^n}{\Delta t} \;=\; \sum_{j\in V(i)} g_{ij}\,(U_{ji}^n - U_i^n) \;+\; \sum_{j\in V(i)} h_{ij}\,(U_{ij}^n - U_i^n) \;+\; e_i U_i^n\,. \quad [44]$$

We observe again that the coefficients g_{ij} and h_{ij} are respectively positive and negative combinations of the unknown, and that e_i vanishes due to the DGCL. Using the expressions of $U_{ij}^n - U_i^n$ and $U_{ji}^n - U_i^n$ given by [37] and [38], we can rewrite [44] in the following form:

$$\frac{U_i^{n+1} \;-\; U_i^n}{\Delta t} \;=\; \sum_{j\in V(i)} \alpha_{ij}(1 - \frac{K_{ji}^0}{2})(U_j^n - U_i^n) + \sum_{j\in V(i)} \beta_{ij}(U_j^n - U_i^n) \quad [45]$$

where α_{ij} and β_{ik} are positive coefficients. As above, according to Lemma 2, we conclude that the ALE scheme satisfies the maximum principle under a CFL condition, provided that $K_{ij}^0 \leq 2$. This last condition is satisfied thanks to the property (P5) of the limiter L, which ends the proof.

3. Density-positive MEV schemes for the Euler equations

The building block for density positivity is flux splitting. We first consider the unidirectional Euler equations and the Godunov exact Riemann solver which is an example of flux difference splitting method that preserves the positivity of ρ under an appropriate CFL condition. Then we derive the multidimensional-CFL condition ensuring that the 2D and 3D schemes involving the unidirectional positive splitting still preserve the positivity of ρ.

3.1. *Unidirectional Euler positive MEV scheme: Godunov's method*

Let us consider the unidirectional formulation of the Euler equations for the usual five variables, applicable to fields which do not depend of y and z:

$$\frac{\partial U}{\partial t}(\mathbf{x},t) + \frac{\partial F(U(\mathbf{x},t))}{\partial x} = 0 \qquad [46]$$

$$U = \begin{pmatrix} \rho \\ \rho u \\ \rho v \\ \rho w \\ e \end{pmatrix} \qquad F(U) = \begin{pmatrix} \rho u \\ \rho u^2 + P \\ \rho u v \\ \rho u w \\ (e+P)u \end{pmatrix} \qquad [47]$$

where (u, v, w) is the velocity and e denotes the total energy per unit area given by $e = \rho\epsilon + \frac{1}{2}\rho(u^2 + v^2 + w^2)$ in which ϵ is the internal energy per unit mass. We restrict the study to the case of an ideal gas, the pressure P being defined through an equation of state $P = (\gamma - 1)\epsilon\rho$ where γ is constant. The general form of an explicit conservative scheme for the Euler equations is:

$$\frac{U_i^{n+1} - U_i^n}{\Delta t} = -\frac{1}{\Delta x}\left(\Phi_{i+1/2}^n - \Phi_{i-1/2}^n\right) , \qquad [48]$$

where U_i^n is the average on the cell $[x_{i-1/2}\ ,\ x_{i+1/2}]$ and $\Phi_{i+1/2}^n = \Phi(U_i^n, U_{i+1}^n)$ denotes the numerical flux approximation of $F(U^n)_{|_{i+1/2}}$. Assuming that ρ and P are positive at time level n, we look for schemes which keep this still true for time level $n+1$. There exists in the literature a lot of flux splittings which enjoy density and pressure positivity, some popular examples are the Boltzman splitting (Perthame *et al.*, 1992) and the HLLE splitting (Einfeldt *et al.*, 1991). In the Godunov method, we solve two independent Riemann problems at each cell interfaces, that do not interact in the cell provided that:

$$\frac{|V_{max}|\ \Delta t}{\Delta x} \leq \frac{1}{2} , \qquad [49]$$

where $|V_{max}|$ denotes the maximum absolute value of the Riemann problem wave speeds. We obtain U_i^{n+1} by averaging:

$$\begin{aligned} U_i^{n+1} \quad = \quad & \\ & \tfrac{1}{\Delta x}\int_{x_{i-\frac{1}{2}}}^{x_i} W_{RP}\left(\tfrac{x - x_{i-\frac{1}{2}}}{\Delta t}, U_{i-1}^n, U_i^n\right) dx + \\ & \tfrac{1}{\Delta x}\int_{x_i}^{x_{i+\frac{1}{2}}} W_{RP}\left(\tfrac{x - x_{i+\frac{1}{2}}}{\Delta t}, U_i^n, U_{i+1}^n\right) dx , \end{aligned} \qquad [50]$$

where W_{RP} is the exact $\rho-$positive solution of the Riemann Problem. This illustrates the well-known fact that under the CFL condition [49] the Godunov scheme preserves the positivity of density.
Let us consider now any unidirectional scheme for the Euler equations, that is $\rho-$positive under a CFL condition:

$$\frac{\Delta t |V_{max}|}{\Delta x} \leq \alpha_1 \qquad [51]$$

where α_1 is a coefficient which depends only on the scheme under study. For example, with Godunov scheme, positivity holds for Courant numbers smaller than $\alpha_1 = 0.5$.

For any arbitrary couple of initial states $U_L = U_i$ and $U_R = U_{i+1}$, the above positivity property can be expressed as a property of the flux between these states. For this we need a third state U_{i-1} to assemble the fluxes around node i. Let us choose it as the mirror state of U_i in x-direction, that is to say $\rho_{i-1}^n = \rho_i^n$, $u_{i-1}^n = -u_i^n$, $v_{i-1}^n = v_i^n$, $w_{i-1}^n = w_i^n$, and $e_{i-1}^n = e_i^n$. The first component Φ_1 of the numerical flux function $\Phi_{i-1/2,1}^n$ should ideally be zero :

$$\Phi_1(U_{i-1}, U_i) = 0 \ \text{ if } \ U_{i-1} \ \text{ is the mirror state of } \ U_i \ . \qquad [52]$$

This property is verified by the three previous refered positive schemes. In particular for the Godunov scheme, due to symmetry reasons, we have: $\Phi^n_{i-1/2,1} = W_{RP,2}(0, U^n_{i-1}, U^n_i) = 0$ where $W_{RP,2}$ denotes the second component of the exact solution W_{RP} of the Riemann problem.

We restrict our study to schemes which satisfy [52]. Then the discretized Equation [48] for the density at node i can be written as:

$$\frac{\rho_i^{n+1} - \rho_i^n}{\Delta t} = -\frac{1}{\Delta x}\Phi^n_{i+1/2,1} \,.$$

Let us denote $\phi^+_{i+1/2} = Max(0, \Phi^n_{i+1/2,1})$ and $\phi^-_{i+1/2} = Min(0, \Phi^n_{i+1/2,1})$, we can write the previous equation as:

$$\rho_i^{n+1} = \left(1 - \frac{\Delta t}{\Delta x}\frac{\phi^+_{i+1/2}}{\rho_i^n}\right)\rho_i^n - \frac{\Delta t}{\Delta x}\phi^-_{i+1/2} \,.$$

For $\rho^n \geq 0$ and under condition [51], ρ^{n+1} is positive. This implies that either $\phi_{i+1/2}$ is negative, or the coefficient of ρ_i^n in right-hand side is positive. Both cases are summed up as follows:

$$\frac{\Delta t \; \phi^+_{i+1/2}}{\rho_i^n \Delta x} \leq 1 \,.$$

Which should hold for the maximum allowed $\Delta t_{max} = \alpha_1 \Delta x / |V_{max}|$. We finally get:

Lemma 5 *An unidirectional scheme that can be written in the form [48], that verifies [52] and that is $\rho-$positive under the CFL condition:*

$$\frac{\Delta t |V_{max}|}{\Delta x} \leq \alpha_1$$

satisfies the following property:

$$\frac{\alpha_1 \; \phi^+_{i+1/2}}{|V_{max}|\rho_i^n} \leq 1 \,. \square \qquad [53]$$

More generally, considering a Riemann problem between two states U_R and U_L, $|V_{max}|$ being the maximum wave speed between these two states, we will say that *a flux splitting Φ is ρ-positive* if there exists α_1 so that:

$$\frac{|V_{max}|\Delta t}{\Delta x} \leq \alpha_1 \quad \text{implies} \quad \frac{\Delta t \, \Phi_1^+(U_L, U_R)}{\rho_L \Delta x} \leq 1 \,. \qquad [54]$$

where Φ_1 is the first component of Φ. For such a flux splitting, we have:

$$\frac{\alpha_1 \; \Phi_1^+(U_L, U_R)}{|V_{max}|\rho_L} \leq 1 \,. \qquad [55]$$

The Godunov, HLLE (Einfeldt *et al.*, 1991) and Perthame (Perthame *et al.*, 1992) schemes involve flux splittings that are ρ-positive according to the above definition. Further, although derived for the x-direction, the previous ρ-positivity statement extends to an arbitrary direction ν (by a rotation of moments and their equations for example). The positivity relation then writes:

$$\frac{\alpha_1 \; \Phi_1^+(U_L, U_R, \nu)}{|V_{max}|\rho_L} \leq 1 \; . \qquad [56]$$

3.2. *First-order positive MEV scheme for the 3D Euler equations*

The three-dimensional Euler model writes classically:

$$\frac{\partial U}{\partial t}(\mathbf{x}, \mathbf{t}) + \frac{\partial F(U(\mathbf{x}, \mathbf{t}))}{\partial \mathbf{x}_1} + \frac{\partial G(U(\mathbf{x}, \mathbf{t}))}{\partial \mathbf{x}_2} + \frac{\partial H(U(\mathbf{x}, \mathbf{t}))}{\partial \mathbf{x}_3} = 0 \qquad [57]$$

with:

$$U = \begin{pmatrix} \rho \\ \rho u \\ \rho v \\ \rho w \\ e \end{pmatrix} \qquad [58]$$

and:

$$F(U) = \begin{pmatrix} \rho u \\ \rho u^2 + P \\ \rho uv \\ \rho uw \\ (e+P)u \end{pmatrix} \quad G(U) = \begin{pmatrix} \rho v \\ \rho uv \\ \rho v^2 + P \\ \rho vw \\ (e+P)v \end{pmatrix} \quad H(U) = \begin{pmatrix} \rho w \\ \rho uw \\ \rho vw \\ \rho w^2 + P \\ (e+P)w \end{pmatrix} \qquad [59]$$

where the pressure is given by $P = (\gamma - 1)\left(e - \frac{1}{2}(u^2 + v^2 + w^2)\right)$. Combining a first-order space-accurate finite-volume discretization of the mass conservation equation combined with a first-order explicit time-integration gives:

$$a_i \rho_i^{n+1} = a_i \rho_i^n - \Delta t \sum_{j \in V(i)} \Phi_1(U_i^n, U_j^n, \nu_{ij}) = a_i \rho_i^n - \Delta t \sum_{j \in V(i)} \phi_{ij} \, l_{ij} \qquad [60]$$

in which $l_{ij} = \left|\left|\nu_{ij}\right|\right| = \left|\left|\int_{\partial\Omega_{ij}} \mu_{ij}(s) \; ds\right|\right|$ with μ_{ij} the unit normal to the boundary $\partial\Omega_{ij}$, Φ is defined as a ρ-positive flux splitting in direction ν_{ij}, and as previously Φ_1 represents the first component of Φ. Therefore, using [56], we successively get:

$$\phi_{ij} \leq \frac{|V_{max}|\rho_i^n}{\alpha_1} \quad , \quad \Delta t \sum_{j \in V(i)} \phi_{ij} l_{ij} \leq \frac{|V_{max}|\rho_i^n \Delta t}{\alpha_1} L_i$$

where $L_i = \sum_{j \in V(i)} l_{ij}$ is the measure of the cell boundary $\partial\Omega_i$. From Equation [60] we finally get that the positivity of ρ_i^{n+1} is ensured when the following condition on the time-step is satisfied:

$$\frac{|V_{max}|\Delta t}{\alpha_1\left(\frac{a_i}{L_i}\right)} \leq 1 \; .$$

Lemma 6 *The three-dimensional first-order space-accurate scheme built from a ρ-positive flux splitting is ρ-positive under the CFL condition:*

$$\frac{|V_{max}|\Delta t}{\left(\frac{a_i}{L_i}\right)} \leq \alpha_1 \; . \qquad [61]$$

REMARK. — The above formula measures the loss with respect to 1D case in positively-stable time step: the ratio $\frac{a_i}{L_i}$ is in general only a fraction of mesh size Δx.

3.3. *High-order positive MEV scheme for the 3D Euler equations*

We now derive *high-order $\rho-$positive schemes* in several dimensions. For sake of clarity we restrict our proof to the 2D case, but it works in a similar way in 3D. We assume that all the ρ_j^n are positive. The general form of the explicit high-order space-accurate scheme governing ρ_i^{n+1} writes:

$$\begin{aligned} a_i\rho_i^{n+1} &= a_i\rho_i^n - \Delta t \sum_{j\in V(i)} \Phi_1(U_{ij}^n, U_{ji}^n, \nu_{ij}) & [62] \\ &= a_i\rho_i^n - \Delta t \sum_{j\in V(i)} \phi_{ij}^{HO} l_{ij} \\ &= a_i\rho_i^n - \Delta t \sum_{j\in V(i)} \left(\frac{\phi_{ij}^{HO+} l_{ij}}{\rho_{ij}^n}\right)\rho_{ij}^n + \left(\frac{\phi_{ij}^{HO-} l_{ij}}{\rho_{ji}^n}\right)\rho_{ji}^n \; , & [63] \end{aligned}$$

where Φ is a ρ-positive flux splitting in direction ν_{ij} and $\phi_{ij}^{HO} = \dfrac{1}{l_{ij}}\Phi_1(U_{ij}^n, U_{ji}^n, \nu_{ij})$ is a flux integration of "high-order" space-accuracy. Following the reconstruction of the solution at the interface $\partial\Omega_{ij}$ given by Equations [37] and [38], ρ_{ij}^n and ρ_{ji}^n write as:

$$\begin{aligned} \rho_{ij}^n &= \rho_i^n + \tfrac{K_{ij}^-}{2}\Big(\epsilon_{ri}(\rho_i^n - \rho_r^n) + \epsilon_{si}(\rho_i^n - \rho_s^n)\Big) \\ \rho_{ji}^n &= \rho_j^n - \tfrac{K_{ji}^0}{2}(\rho_j^n - \rho_i^n) \end{aligned} \qquad [64]$$

where K_{ij}^-, K_{ji}^0, ϵ_{ri} and ϵ_{si} are positive. First, we can notice that ρ_{ij}^n and ρ_{ji}^n are positive. Indeed, according to [15] and [16] we can also write ρ_{ij}^n as:

$$\rho_{ij}^n = \rho_i^n + \frac{1}{2}L_{ij}(\rho^n) = \rho_i^n + \frac{K_{ij}^0}{2}\Delta^0\rho_{ij}^n = \rho_i^n + \frac{K_{ij}^0}{2}(\rho_j^n - \rho_i^n) \qquad [65]$$

where K^0_{ij} is positive. As the property (P5) of the limiter implies $K^0_{ij} \leq 2$ and $K^0_{ji} \leq 2$, we deduce from Equations [64] and [65] that

$$min(\rho^n_i,\ \rho^n_j) \leq \rho^n_{ij},\ \rho^n_{ji} \leq max(\rho^n_i,\ \rho^n_j)$$

so that ρ^n_{ij} and ρ^n_{ji} are positive. Using [64], we can rewrite the discrete Equation [63] as follows:

$$\rho_i^{n+1} = \sum_{j\in V(i)} \alpha_{ij}\rho^n_j +$$

$$\rho^n_i\left(1 - \frac{\Delta t}{a_i}\sum_{j\in V(i)}\left(\frac{\phi^{HO+}_{ij} l_{ij}}{\rho_{ij^n}}\right)(1 + K^-_{ij}\frac{\epsilon_{ri}+\epsilon_{si}}{2}) + \frac{\Delta t}{a_i}\sum_{j\in V(i)}\left(-\frac{\phi^{HO-}_{ij} l_{ij}}{\rho^n_{ji}}\right)\frac{K^0_{ji}}{2}\right) \tag{66}$$

where α_{ij} are positive since $K^0_{ji} \leq 2$ as already seen. We deduce that the positivity of ρ is preserved under the following condition on Δt:

$$\frac{\Delta t}{a_i}\sum_{j\in V(i)}\left(\frac{\phi^{HO+}_{ij} l_{ij}}{\rho_{ij^n}}\right)(1 + K^-_{ij}\frac{\epsilon_{ri}+\epsilon_{si}}{2}) \leq 1\ . \tag{67}$$

In the above equation, the mesh dependant quantity $M_{ij} = \epsilon_{ri} + \epsilon_{si}$ can be written as:

$$M_{ij} = \frac{l_j^2}{l_s l_r}\left(\frac{l_r\sin\theta_r + l_s\sin\theta_s}{l_j\sin\theta}\right)$$

where θ_r, θ_s and θ_t are defined as in Figure 4 and l_p denotes the length of the vector **ip** for $p = r, s$ or j. Given $M_i = \max_j M_{ij}$, the CFL condition [67] ensuring the positivity of ρ is satisfied when:

$$\frac{\Delta t}{a_i}\sum_{j\in V(i)}\left(\frac{\phi^{HO+}_{ij} l_{ij}}{\rho_{ij^n}}\right) \leq \frac{1}{1+M_i}\ . \tag{68}$$

since $K^-_{ij} \leq 2$ thanks to the properties (P1) and (P5) of the limiter L. On the other hand, we have $\phi^{HO}_{ij} = \frac{1}{l_{ij}}\Phi_1(U^n_{ij}, U^n_{ji}, \nu_{ij})$ with Φ a ρ-positive flux splitting, so that we get according to [56]:

$$\frac{\alpha_1\phi^{HO+}_{ij}}{|V_{max}|\rho_{ij}} \leq 1\ . \tag{69}$$

Given $L_i = \sum_{j\in V(i)} l_{ij}$ the measure of the cell boundary $\partial\Omega_i$, from Equations [68] and [69] we derive a positivity statement for a class of high-order schemes, that we write for simplicity for the previous third-order scheme :

Lemma 7 *The quasi third-order scheme introduced in Section 2, see Equations [15][16] and [17], based on a ρ-positive flux splitting [54] is ρ-positive under the CFL condition:*

$$\frac{\Delta t\,|V_{max}|}{\left(\frac{ai}{L_i}\right)} \leq \frac{\alpha_1}{1+M_i}\ . \tag{70}$$

In the ALE case, the model [59] is modified in a manner that is similar to the scalar conservation law case. For the spatial discretisation, the Riemann solver is modified by the term involving the mesh velocity, but its positivity property is unchanged. Also, the time derivative $d\Big(a_i(t)U_i(t)\Big)/dt$ is now approximated by $(a_i^{n+1}\rho_i^{n+1} - a_i^n\rho_i^n)/\Delta t$, and Equation [66] becomes:

$$\frac{a_i^{n+1}}{a_i^n}\,\rho_i^{n+1} \;=\; \sum_{j\in V(i)} \alpha_{ij}\rho_j^n \;+$$

$$\rho_i^n\left(1-\frac{\Delta t}{a_i^n}\sum_{j\in V(i)}\left(\frac{\phi_{ij}^{HO+}l_{ij}}{\rho_{ij^n}}\right)(1+K_{ij}^{-}\frac{\epsilon_{ri}+\epsilon_{si}}{2})+\frac{\Delta t}{a_i^n}\sum_{j\in V(i)}\left(-\frac{\phi_{ij}^{HO-}l_{ij}}{\rho_{ji}^n}\right)\frac{K_{ji}^0}{2}\right)$$

where α_{ij} are positive, so that we can derive the same ρ-positivity statement than for the fixed grids case.
REMARK. — We observe that the DGCL is not necessary for the positivity of ρ with the ALE formulation.

4. Maximum principle for the mass fractions in multi-component flows

We consider now a compressible multi-component flow. Larrouturou derived in (Larrouturou, 1991) a scheme that preserves the maximum principle for the mass fractions for 1D first-order and second-order schemes and for 2D first-order schemes. In this section, we extend Larrouturou's method and results to multidimensional second-order schemes.

4.1. *First-order multidimensional MEV scheme*

First, we recall the two-component Euler equations in three-dimensions:

$$\frac{\partial U}{\partial t}(\mathbf{x},\mathbf{t}) + \frac{\partial F(U(\mathbf{x},\mathbf{t}))}{\partial \mathbf{x}_1} + \frac{\partial G(U(\mathbf{x},\mathbf{t}))}{\partial \mathbf{x}_2} + \frac{\partial H(U(\mathbf{x},\mathbf{t}))}{\partial \mathbf{x}_3} = 0 \qquad [71]$$

$$U = \begin{pmatrix} \rho \\ \rho u \\ \rho v \\ \rho w \\ e \\ \rho Y \end{pmatrix} \qquad [72]$$

$$F(U) = \begin{pmatrix} \rho u \\ \rho u^2 + P \\ \rho uv \\ \rho uw \\ (e+P)u \\ \rho uY \end{pmatrix} \quad G(U) = \begin{pmatrix} \rho v \\ \rho uv \\ \rho v^2 + P \\ \rho vw \\ (e+P)v \\ \rho vY \end{pmatrix} \quad H(U) = \begin{pmatrix} \rho w \\ \rho uw \\ \rho vw \\ \rho w^2 + P \\ (e+P)w \\ \rho wY \end{pmatrix} \qquad [73]$$

where we use the notations given in Section 3, except that Y is the mass fraction of the first passive species (and $1 - Y$ that of the second one). The explicit conservative discretization of the problem is given by:

$$a_i \, \frac{U_i^{n+1} - U_i^n}{\Delta t} = - \sum_{j \in V(i)} \Phi(U_i^n, U_j^n, \nu_{ij}) = - \sum_{j \in V(i)} \Phi_{ij}^n \qquad [74]$$

Larrouturou's idea is to evaluate the first five components of the numerical flux function ($\Phi_{ij,\alpha}^n$ for $\alpha = 1..5$) with a classical Godunov-type scheme and the last component of the numerical flux $\Phi_{ij,6}^n$ is defined as follows:

$$\Phi_{ij,6}^n = \Phi_{ij,1}^{n+} Y_i^n + \Phi_{ij,1}^{n-} Y_j^n \ . \qquad [75]$$

With this construction and under a CFL-like condition, the scheme preserves the maximum principle for the mass fraction Y, see (Larrouturou, 1991). In his argument, Larrouturou needs to assume that the positivity of ρ is preserved and introduces an extra condition on the time-step. Here, we show the following lemma

Lemma 8 *If the first five components of the flux are evaluated with a first-order space-accurate scheme built from a ρ-positive flux splitting , then no extra CFL condition (than the one required for the ρ-positivity of the scheme) is actually needed to ensure the preservation of the maximum principle for the mass fraction.*

Proof: we denote $\phi_{ij} = \frac{1}{l_{ij}} \Phi_{ij,1}^n$, so that we can write the discretized equations for ρ and ρY in the following form:

$$\left\{ \begin{array}{rcl} \rho_i^{n+1} & = & \rho_i^n - \Delta t \displaystyle\sum_{j \in V(i)} \left(\frac{l_{ij}}{a_i} \right) \phi_{ij} \\ \rho_i^{n+1} Y_i^{n+1} & = & \rho_i^n Y_i^n - \Delta t \displaystyle\sum_{j \in V(i)} \left(\frac{l_{ij}}{a_i} \right) \left(\phi_{ij}^+ \, Y_i^n + \phi_{ij}^- \, Y_j^n \right) \end{array} \right.$$

We know that ρ_i^{n+1} is positive. Therefore we can rewrite the last equation as:

$$\begin{aligned} Y_i^{n+1} &= \left(\frac{\rho_i^n - \Delta t \displaystyle\sum_{j \in V(i)} \phi_{ij}^+ \big(\frac{l_{ij}}{a_i}\big)}{\rho_i^n - \Delta t \displaystyle\sum_{j \in V(i)} \phi_{ij} \big(\frac{l_{ij}}{a_i}\big)} \right) Y_i^n \\ &\quad + \sum_{j \in V(i)} \left(\frac{-\phi_{ij}^- \Delta t \big(\frac{l_{ij}}{a_i}\big)}{\rho_i^n - \Delta t \displaystyle\sum_{j \in V(i)} \phi_{ij} \big(\frac{l_{ij}}{a_i}\big)} \right) Y_j^n \\ &= \alpha_i Y_i^n + \sum_{j \in V(i)} \alpha_{ij} Y_j^n \,. \end{aligned} \quad [76]$$

We will prove now that the coefficients α_i and α_{ij} are positive. We can first notice that:

$$\rho_i^n - \Delta t \sum_{j \in V(i)} \phi_{ij} \left(\frac{l_{ij}}{a_i} \right) = \rho_i^{n+1} > 0 \,. \quad [77]$$

On the other hand, as Φ is a ρ-positive flux splitting, with the positivity condition [56], we get:

$$\phi_{ij}^+ \leq \frac{\rho_i^n |V_{max}|}{\alpha_1}$$

so that:

$$\Delta t \sum_{j \in V(i)} \phi_{ij}^+ l_{ij} \leq \frac{\rho_i^n |V_{max}| \Delta t}{\alpha_1} L_i$$

where L_i is defined as previously. Then the CFL condition [61] implies:

$$\Delta t \sum_{j \in V(i)} \phi_{ij}^+ l_{ij} \leq \rho_i^n a_i \,. \quad [78]$$

From [77] and [78], we deduce that all the coefficients α_i and α_{ij} in [76] belong to $[0, 1]$. Therefore, Y_i^{n+1} is a convex combination of the Y_j^n, $j = i$ or $j \in V(i)$, since $\alpha_i + \sum_{j \in V(i)} \alpha_{ij} = 1$, so that the maximum principle is preserved. $\square$

4.2. *A high-order 2D/3D multi-component MEV scheme*

We now wish to obtain the maximum principle for high-order schemes. For this purpose, we consider a high-order solver for the Euler equations based on a ρ-positive flux splitting, and therefore, which preserves the positivity of ρ under a CFL condition (see Section 3.3). For sake of clarity, we restrict our proof to 2D. Using the same notations than in the previous section, the discretized equation for ρ and ρY are now written:

$$\left\{\begin{array}{rcl} \rho_i^{n+1} & = & \rho_i^n - \Delta t \displaystyle\sum_{j\in V(i)} \phi_{ij}^{HO}\left(\frac{l_{ij}}{a_i}\right) \\ \rho_i^{n+1} Y_i^{n+1} & = & \rho_i^n Y_i^n - \Delta t \displaystyle\sum_{j\in V(i)} \left(\phi_{ij}^{HO+} Y_{ij}^n + \phi_{ij}^{HO-} Y_{ji}^n\right)\left(\frac{l_{ij}}{a_i}\right). \end{array}\right.$$

Then, similarly to [76], we get:

$$\begin{array}{l} Y_i^{n+1} = \\ \qquad \left(\dfrac{\rho_i^n Y_i^n - \Delta t \displaystyle\sum_{j\in V(i)} \phi_{ij}^{HO+}\left(\frac{l_{ij}}{a_i}\right) Y_{ij}^n}{\rho_i^n - \Delta t \displaystyle\sum_{j\in V(i)} \phi_{ij}^{HO}\left(\frac{l_{ij}}{a_i}\right)}\right) + \\ \qquad \displaystyle\sum_{j\in V(i)} \left(\dfrac{(-\phi_{ij}^{HO-})\Delta t\left(\frac{l_{ij}}{a_i}\right)}{\rho_i^n - \Delta t \displaystyle\sum_{j\in V(i)} \phi_{ij}^{HO}\left(\frac{l_{ij}}{a_i}\right)}\right) Y_{ji}^n\,. \end{array} \qquad [79]$$

We use here the quasi third-order limited reconstruction introduced in Section 2.4:

$$\left\{\begin{array}{rcl} Y_{ij}^n & = & Y_i^n + \frac{K_{ij}^-}{2}\Big(\epsilon_{si}(Y_i^n - Y_s^n) + \epsilon_{ri}(Y_i^n - Y_r^n)\Big) \\ Y_{ji}^n & = & Y_j^n - \frac{K_{ji}^0}{2}(Y_j^n - Y_i^n). \end{array}\right. \qquad [80]$$

If we compare [79] and [80] to [76], we observe that the new terms Y_{ij}^n and Y_{ji}^n are differences between Y_l^n and Y_i^n plus respectively Y_i^n and Y_j^n, so that the total weight is unchanged compared to [76] and equal to 1. It remains to check that each coefficient is positive. Now we rewrite Equation [79] as:

$$\begin{array}{rl} Y_i^{n+1} = & \\ & \dfrac{Y_i^n}{\rho_i^{n+1}}\left(\rho_i^n - \Delta t \displaystyle\sum_{j\in V(i)} \phi_{ij}^{HO+}\left(1 + \frac{K_{ij}^-}{2}(\epsilon_s + \epsilon_r)\right)\left(\frac{l_{ij}}{a_i}\right)\right) + \\ & \dfrac{Y_i^n}{\rho_i^{n+1}}\left(\Delta t \displaystyle\sum_{j\in V(i)} (-\phi_{ij}^{HO-})\frac{K_{ji}^0}{2}\left(\frac{l_{ij}}{a_i}\right)\right) + \\ & \dfrac{\Delta t}{\rho_i^{n+1}} \displaystyle\sum_{j\in V(i)} \phi_{ij}^{HO+}\left(\frac{l_{ij}}{a_i}\right)\left(\frac{K_{ij}^-\epsilon_{si}}{2} Y_s^n + \frac{K_{ij}^-\epsilon_{ri}}{2} Y_r^n\right) + \\ & \dfrac{\Delta t}{\rho_i^{n+1}} \displaystyle\sum_{j\in V(i)} (-\phi_{ij}^{HO-})(1 - \frac{K_{ji}^0}{2})\left(\frac{l_{ij}}{a_i}\right) Y_j^n. \end{array} \qquad [81]$$

Here, vertices s and r are defined in relation with vertex j, but we have chosen to not complicate the notations. From the positivity condition [56] and the CFL condition

[70] ensuring the positivity of ρ, we deduce as previously that all the coefficients of this Y-splitting are non-negative. We have observed that the total weight is again equals to 1. Therefore, Y_i^{n+1} can be written as a convex linear combination of Y_j^n, $j \in V(i)$ or $j = i$, and the maximum principle is thus preserved with no extra CFL condition.

We finish this section by examining the ALE case. In that case, [79] just tranforms into:

$$\begin{aligned} Y_i^{n+1} \quad = & \\ & \left(\frac{(\frac{a_i^n}{a_i^{n+1}})\rho_i^n Y_i^n - \Delta t \sum_{j \in V(i)} \phi_{ij}^{HO+}(\frac{l_{ij}}{a_i^{n+1}}) Y_{ij}^n}{(\frac{a_i^n}{a_i^{n+1}})\rho_i^n - \Delta t \sum_{j \in V(i)} \phi_{ij}^{HO}(\frac{l_{ij}}{a_i^{n+1}})} \right) + \\ & \sum_{j \in V(i)} \left(\frac{(-\phi_{ij}^{HO-})\Delta t(\frac{l_{ij}}{a_i^{n+1}})}{(\frac{a_i^n}{a_i^{n+1}})\rho_i^n - \Delta t \sum_{j \in V(i)} \phi_{ij}^{HO}(\frac{l_{ij}}{a_i^{n+1}})} \right) Y_{ji}^n \end{aligned} \qquad [82]$$

and the same barycenter argument still applies.

REMARK. — We observe that the DGCL is not necessary for species maximum principle with the ALE formulation.

REMARK. — In the case of a viscous flow, a particular attention has to be paid to the discrete diffusion operators that should also preserve positivity of species; for finite element discretization, this is related to standard acute angle condition, see (Baba *et al.*, 1981).

REMARK. — All the previous results can be easily extended to boundary for various boudary conditions by applying mirror principles.

5. Some numerical results

The theoretical results presented in this paper have three types of consequence on software. Firstly, the extra robustness of the upwind-element method with respect to the nodal gradient method gets a theoretical confirmation. Secondly, for the explicit upwind-element scheme, a nonlinear stability condition is available for software in order to get more robustness than standard time-step length evaluations relying on unproved extensions of linear and scalar heuristics. Thirdly, with the proposed methodology, we can introduce and limit new higher-order schemes in such a way that density positivity holds. The resulting robustness has been abundantly illustrated by high Mach calculations in several papers, such as (Stoufflet *et al.*, 1996) and papers

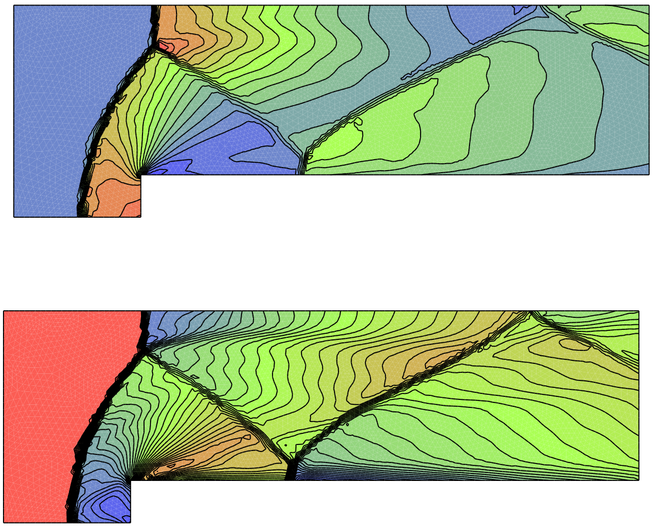

Figure 6. *Mach 3 unsteady forward step case, with the present method combined with HO5 scheme: 22 density contours , min ρ = 0.75, max ρ = 6.25,* $\Delta\rho = 0.25$, *40 Mach contours, min M = 0., max M = 3.,* $\Delta M = 0.075$

referenced in it. The high Mach calculations presented in (Stoufflet *et al.*, 1996) were not possible with previous versions of the schemes (*i.e.* without the upwind elements). Instead of presenting more high Mach flow calculations, we show in this section that the new limited scheme is useful for transonic flow simulations since it represents a good compromise between robustness and accuracy.

The first numerical experiment is a classical 2D test case, the transient flow around a forward step for a farfield Mach number set to 3. The mesh corresponds to the unstructured triangulation used in (Abgrall, 1994) (less than 5000 nodes). The low-dissipation flux HO5 (see [18]) is applied. Explicit time advancing is performed with the three-stage Shu-Osher scheme ((Shu *et al.*, 1988)). A time-step slighty larger than predicted by our analysis could be used without unstability. The Mach number and density contours at time $T = 4.$ are depicted in Figure 6. The results are very clean, with a reasonable level of numerical dissipation, since they seem quite close to those obtained with the third-order ENO scheme of Abgrall, this latter scheme being not constrained by strict density positivity.

Two 3D applications are then considered in order to illustrate the gain obtained in accuracy when the standard second-order scheme equipped with van Albada limiter as in (Stoufflet *et al.*, 1996) is replaced by limiter [16] combined with the HO5 flux (see [18]). In both case an implicit BDF2 time advancing is used.

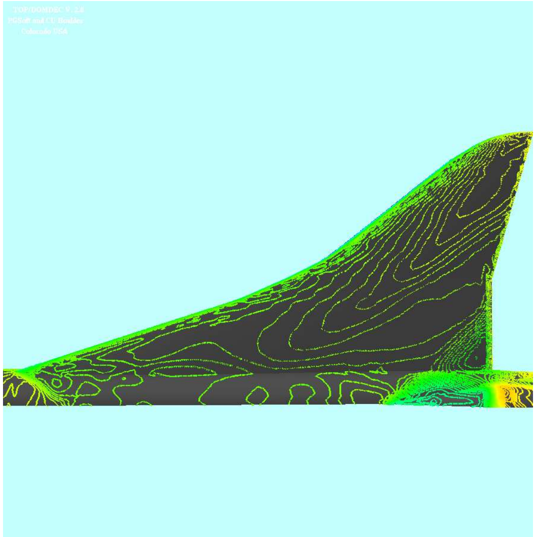

Figure 7. *Flow around Dassault SSBJ geometry, Mach 1.6, incidence 0: Mach number contours on upper side obtained by applying the previous version of the scheme*

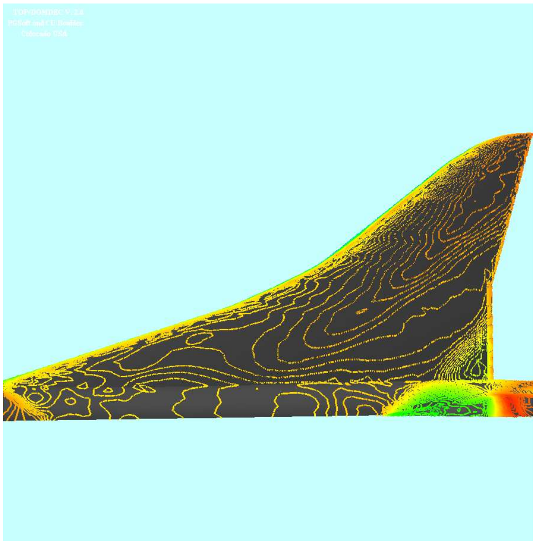

Figure 8. *Flow around Dassault SSBJ geometry, Mach 1.6, incidence 0: Mach number contours on upper side obtained by applying the new version of the scheme*

The first 3D example concerns the calculation of the inviscid steady flow around a supersonic jet geometry at a farfield Mach number set to 1.6 and an angle of attack of 0 degree. The unstructured tetrahedral mesh involves 170000 vertices, which represents a medium-fine mesh for this geometry. In Figures 7 and 8, we depict the Mach number isolines on the upper surface of the wing-body set for the standard second-order scheme and the new higher-order one, respectively. The comparison of both results shows rather important differences, with extremas predicted at different locations on the geometry and more flow details captured by the higher-order scheme. Using scheme [16][18] produces an improvement of 4% for the drag (from 15940 to 15313) and of 2% for the lift (from 120690 to 123345).

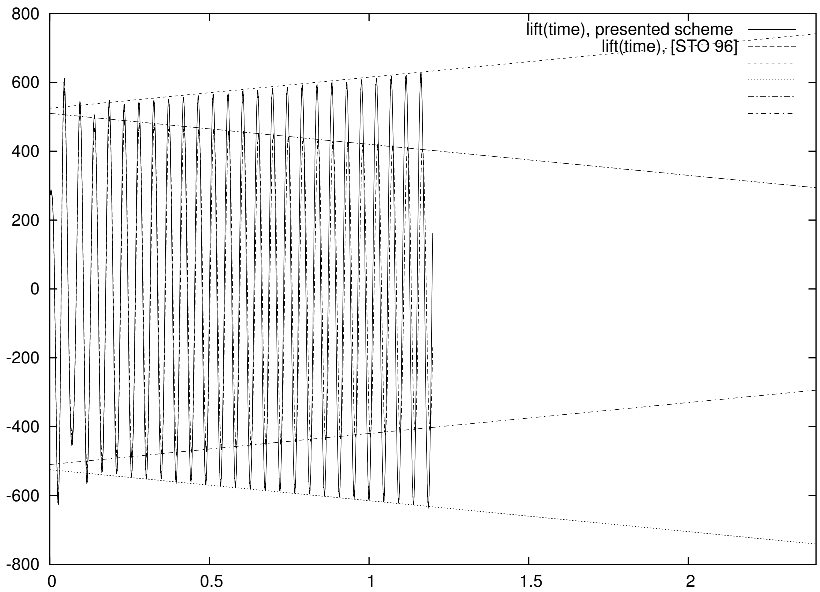

Figure 9. *Flutter of the Agard Wing 445.6 underlined by the amplitude of the lift oscillation as a function of time. Dashes: the previous version (Stoufflet* et al.*, 1996) of the scheme is applied, the initial oscillation is damped. Line: scheme [16][18] is applied, oscillations are consistently amplified with the experimental results*

The second 3D example concerns the simulation of an unsteady inviscid flow involving mesh deformations. We consider a rather standard flutter test case: the flutter of the AGARD Wing 445.6 which has been measured with various flow conditions by Yates (Yates, 1987). We focus on a rather tricky transonic case, for which the farfield Mach number is 1.072. More precisely, the reference density is set to $9.838\ 10^{-8}\ \ slugs/inch^3$ and the reference pressure to $16.8\ \ slugs/(inch.sec^2)$. According to the experimental results detailed in (Yates, 1987), the flow conditions are inside the unstability domain and the wing flutter is already pronounced.
The three-dimensional unstructured tetrahedral CFD mesh contains 22014 vertices. For the aeroelastic analysis, the structure of the wing is discretized by a thin plate finite element model which contains 800 triangular composite shell elements and is based on the informations given in (Yates, 1987).

This transient aeroelastic case is computed with the fluid-structure interaction methodology developed by Farhat and co-workers, see (Farhat, 1995). We compare again the scheme defined in (Stoufflet *et al.*, 1996) to scheme [16][18]. The time step is defined according to a maximum fluid Courant number of 900. In Figure 9, we depict the wing lift coefficient as a function of time. With the new scheme, the flutter amplification is well predicted consistently with the experimental results while an important damping is predicted with the previous scheme leading to erroneous results.

6. Conclusion

This work focuses on the positivity of Mixed-Element-Volume upwind schemes. This family, based on linear finite-element approximation, is identified by a few main features, in particular vertex centering, which leads to the smallest number of unknowns for a given mesh and the possibility to assemble the fluxes on an edge-based mode. We propose an analysis for defining a positive sub-family of MUSCL-based second-order accurate schemes. Three types of positivity are examined: maximum principle for a scalar nonlinear conservation law, density positivity for the Euler equations, and maximum principle for convected species in a multi-component flow. In each of the three cases, the proposed analysis is extended to moving mesh ALE approximations. In particular we extend to second-order accuracy the contribution of (Farhat *et al.*, 2001). We also *a posteriori* state, as a particular case, the robustness of the upwind-element scheme used in (Stoufflet *et al.*, 1996) which was derived empirically for the special treatment of very stiff flows, involving strong bow shocks at large Mach numbers.

In the case of explicit time advancing, this analysis brings a rigorous time-step evaluation for positivity. With this analysis, we have also defined new schemes that are as robust but less dissipative than the previous basic upwind-element scheme, because the conditions for positiveness are accurately identified.

The numerical study presented in this paper highlights the benefits that can be acquired when these new schemes are applied. With the new spatial discretization schemes presented in this work, steady and unsteady flow calculations show thin and monotone shock structures, and a lower amount of numerical dissipation compared to the previous MEV schemes. It should be noted that dissipation can be even more decreased by adding sensors dedicated to the inhibition of limiters in regions where the flow is regular. The improvement in control of both monotony and dissipation is finally demonstrated by computing a rather critical flutter case for which the scheme accuracy is a determining factor on qualitative outputs.

Acknowledgements

The present work was inspired by both Bram Van Leer's and Anthony Jameson's works. The supersonic jet geometry was kindly provided by Dassault-Aviation. The authors thank the Centre Informatique National de l'Enseignement Supérieur (CINES) for providing the computational resources. They also thank Stephen Wornom for various suggestions and comments on this paper.

7. References

Abgrall R., " On essentially non-oscillatory schemes on unstructured meshes, analysis and implementation", *Journal of Computational Physics*, vol. 114, p. 45-58, 1994.

Abgrall R., " How to prevent pressure oscillations in multicomponent flows: a quasi conservative approach", *Journal of Computational Physics*, vol. 125, p. 150-160, 1996.

Arminjon P., Dervieux A., " Construction of TVD-like artificial viscosities on two-dimensional arbitrary FEM grids", *Journal of Computational Physics*, vol. 106, p. 106, No 1, 176-198, 1993.

Arminjon P., Viallon M., " Convergence of a finite volume extension of the Nessyahu-Tadmor scheme on unstructured grids for a two-dimensional linear hyperbolic equation", *SIAM J. Num. Analysis*, vol. 36, n° 3, p. 738-771, 1999.

Baba K., Tabata M., " On a conservative upwind finite element scheme for convective diffusion equations", *R.A.I.R.O Numer. Anal.*, vol. 15, p. 3-25, 1981.

Camarri S., Koobus B., Salvetti M.-V., Dervieux A., " A low-diffusion MUSCL scheme for LES on unstructured grids", *Computers and Fluids*, vol. 33, p. 1101-1129, 2004.

Catalano L. A., " A new reconstruction scheme for the computation of inviscid compressible flows on 3D unstructured grids", *International Journal for Numerical Methods in Fluids*, vol. 40, n° 1-2, p. 273-279, 2002.

Cockburn B., Shu C.-W., " TVB Runge-Kutta local projection discontinuous Galerkin finite element method for conservation laws II: General framework", *Mathematics of Computation*, vol. 52, p. 411-435, 1989.

Debiez C., Approximation et linéarisation d'écoulements aérodynamiques instationnaires, PhD thesis, University of Nice, France (in French), 1996.

Debiez C., Dervieux A., Mer K., Nkonga B., " Computation of Unsteady Flows with Mixed Finite Volume/Finite Element Upwind Methods", *International Journal for Numerical Methods in Fluids*, vol. 27, p. 193-206, 1998.

Deconinck H., Roe P., Struijs R., " A Multidimensional Generalization of Roe's Flux Difference Splitter for the Euler Equations", *Computers and Fluids*, vol. 22, n° 23, p. 215-222, 1993.

Einfeldt B., Munz C. D., Roe P. L., Sjogreen B., " On Godunov-type methods near low densities", *Journal of Computational Physics*, vol. 92, p. 273-295, 1991.

Farhat C., High performance simulation of coupled nonlinear transient aeroelastic problems, Special course on parallel computing in CFD. n° R-807, NATO AGARD Report, October, 1995.

Farhat C., Geuzaine P., Grandmont C., " The Discrete Geometric Conservation Law and the nonlinear stability of ALE schemes for the solution of flow problems on moving grids", *J. of Computational Physics*, vol. 174, p. 669-694, 2001.

Farhat C., Lesoinne M., " Two efficient staggered procedures for the serial and parallel solution of three-dimensional nonlinear transient aeroelastic problems", *Comput. Meths. Appl. Mech. Engrg.*, vol. 182, p. 499-516, 2000.

Fezoui L., Dervieux A., Finite-element non oscillatory schemes for compressible flows, Symposium on Computational Mathematics and Applications n° 730, Publications of university of Pavie (Italy), 1989a.

Fezoui L., Stoufflet B., " A class of implicit schemes for Euler simulations with unstructured meshes", *Journal of Computational Physics*, vol. 84, n° 1, p. 174-206, 1989b.

Godlewski E., Raviart P.-A., *Numerical approximation of hyperbolic systems of conservation law*, Springer, 1996.

Harten A., " High resolution schemes for hyperbolic conservation laws", *Journal of Computational Physics*, vol. 49, p. 357-393, 1983.

Harten A., Engquist B., Osher S., Chakravarthy S., " Uniformly high-order accurate essentially non oscillatory schemes, III", *Journal of Computational Physics*, vol. 71, p. 231-303, 1987.

Jameson A., Artificial Diffusion, Upwind Biasing, Limiters and their Effect on Accuracy and Multigrid Convergence in Transonic and Hypersonic Flows, AIAA paper 93-3359, 1993.

Larrouturou B., " How to Preserve the Mass Fraction Positivity when Computing Compressible Multi-component Flows", *Journal of Computational Physics*, vol. 95, p. 59-84, 1991.

Linde T., Roe P., On multidimensional positively conservative high resolution schemes, AIAA paper 97-2098, 1998.

Mer K., " Variational analysis of a mixed element/volume scheme with fourth-order viscosity on general triangulations", *Computer Methods in Applied Mechanics and Engineering*, vol. 153, p. 45-62, 1998.

Murrone A., Guillard H., " A five equation model for compressible two-phase flow computations", *Journal of Computational Physics*, vol. 202, n° 2, p. 664-698, 2005.

Perthame B., Khobalate B., Maximum Principle on the Entropy and Minimal Limitations for Kinetic Scheme, Rapport de recherche n° 1628, INRIA, 1992.

Perthame B., Shu C., " On positivity preserving finite-volume schemes for Euler equations", *Numerical Mathematics*, vol. 73, p. 119-130, 1996.

Piperno S., Depeyre S., " Criteria for the Design of Limiters yielding efficient high resolution TVD schemes", *Comput. & Fluids*, vol. 27, n° 2, p. 183-197, 1998.

Selmin V., Formaggia L., " Unified construction of finite element and finite volume discretizations for compressible flows", *International Journal for Numerical Methods in Engineering*, vol. 39, n° 1, p. 1-32, 1998.

Shu C., Osher S., " Efficient Implementation of Essential Non-oscillatory Shock Capturing Schemes", *Journal of Computational Physics*, vol. 77, p. 439-471, 1988.

Sidilkover D., A Genuinely Multidimensional Upwind Scheme and Efficient Multigrid Solver for the Compressible Euler Equations, ICASE report no. 94-84, 1994.

Stoufflet B., Periaux J., Fezoui L., Dervieux A., 3-D Hypersonic Euler Numerical Simulation around Space Vehicles using Adapted Finite Elements, 25th AIAA Aerospace Meeting, Reno (1987), AIAA paper 86-0560, 1996.

Sweby P. K., " High resolution schemes using limiters for hyperbolic conservation laws", *SIAM Journal in Numerical Analysis*, vol. 21, p. 995-1011, 1984.

Van Leer B., " Towards the Ultimate Conservative Difference Scheme V: A Second Order Sequel to Godunov's Method", *Journal of Computational Physics*, vol. 32, p. 101-136, 1979.

Venkatakrishnan V., “ A perspective on unstructured grid flow solvers”, *AIAA Journal*, vol. 34, p. 533-547, 1996.

Venkatakrisnan V. *et al.*, “ Barriers and Challenges in CFD”, *ICASE Workshop, Kluwer Acad. Pub., ICASE/LaRC Interdisciplinary Series*, vol. 6, p. 299-313, 1998.

Whitaker D., Grossman B., Löhner R., Two-Dimensional Euler Computations on a Triangular Mesh Using an Upwind, Finite-Volume Scheme, AIAA paper 89-0365, 1989.

Yates E., “ AGARD standard aeroelastic configuration for dynamic response, candidate configuration I. - Wing 445.6”, *NASA TM-100492*, 1987.